

# SYNTHETIC ABSORPTION LINES IN COOL STARS AND NORMAL GALAXIES

B. Barbuy

Instituto Astronômico e Geofísico, Univ. de São Paulo, Brazil

## RESUMEN

Describimos primero las bases de los cálculos de síntesis espectral donde se introducen listas de líneas con constantes atómicas y moleculares. Se discute también la exactitud de los modelos actuales de atmósferas.

Se describe la aplicación de espectros sintéticos para reproducir los espectros de diferentes objetos. Se muestra la derivación de cocientes de elementos y de isótopos y se incluye una discusión de los resultados para carbono, nitrógeno y oxígeno. Se describe el estudio de espectros de estrellas T Tauri develadas, donde se pueden usar las bandas moleculares para verificar los parámetros estelares.

Se describe una malla de 700 espectros sintéticos que incluye estrellas de referencia que se usa con un método de perturbación para estudiar poblaciones estelares.

Finalmente se presentan cálculos de los rasgos intensos en espectros compuestos, y en particular, de las líneas del triplete de MgI, las líneas del triplete de CaII, y las bandas de TiO en cúmulos globulares ricos en metales y en galaxias S0/E.

## ABSTRACT

We first describe the basis of spectrum synthesis calculations where line lists with atomic and molecular constants are introduced. The accuracy of present-day available model atmospheres is also discussed.

The application of synthetic spectra to reproduce the spectra of different objects is then described: The derivation of elemental and isotopic ratios is shown, including a discussion on results for the carbon, nitrogen and oxygen elements. The study of de-veiled spectra of T Tauri stars is described, where molecular bands can be used to check stellar parameters.

A grid of 700 synthetic spectra together with reference stars, used through a perturbation method to study stellar populations is described.

Finally the reproduction of strong features in composite spectra, and in particular, the MgI triplet lines, the CaII triplet lines, and TiO bands in metal-rich globular clusters and S0/E galaxies is given.

**Key words:** STARS - ABUNDANCES — GALAXIES - STELLAR CONTENT

## 1. Introduction

Spectrum synthesis consists in reproducing theoretically the observed flux (or spectra) of stars.

A great accuracy in these calculations are reached nowadays due to a combination of:

(1) Observations obtained with high quantum efficiency and high resolution; (2) Powerful computing permitting the computation of model atmospheres and line lists.

As a result of the application of well-known physics to accurate and extensive computations, combined to high quality observed spectra, it is possible to derive accurate elemental abundances in stars, and to reproduce the spectra of galaxies.

## 2. Spectrum synthesis

The monochromatic flux is computed through the classical formula:

$$F_{\lambda} = 2 \int_0^{\infty} B_{\lambda}(T) E_2(\tau_{\lambda}) d\tau_{\lambda}$$

For practical purposes, the temperature distribution is given as a function of a reference optical depth scale  $\tau_o$ , in general  $\tau_{5000\text{\AA}}$ , so that

$$F_{\lambda} = 2 \int_{-\infty}^{\infty} B_{\lambda}(T) E_2(\tau_{\lambda}) \frac{l_{\lambda} + k_{\lambda}}{\kappa_o} \frac{d \log \tau_o}{\log e}$$

where  $l_{\lambda}$  = line absorption coefficient and  $k_{\lambda}$  = continuous absorption coefficient.

### 2.1 Continuous absorption coefficient

Note that the calculation of the line is in fact a ratio of line absorption to continuous absorption coefficients  $l_{\lambda}/\kappa_o$ . The appropriate calculation of the continuum is therefore important.

We list below the mechanisms taken into account by Kurucz (1979, 1992), Plez et al (1992) and Spite (1967); we point out that Kurucz extends his calculations to stellar effective temperatures of 50.000 K, and therefore includes higher ionized atoms:

Kurucz : HI-II, HeI-III, CI-IV, NII-V, OII-VI, NeI-VI, MgI, AlI, SiI,  $H_2^+$ ,  $H^-$ ,  $H_2^-$ , H and He Rayleigh scattering, electron scattering.

Plez et al: H,  $H^-$ ,  $H_2^-$ ,  $H_2^+$ , He,  $He^-$ , CI, MgI, AlI, SiI, scattering by H,  $H_2$ , and electrons In the opacity calculations are included the molecules of TiO, CO, CN,  $C_2$ , HCN,  $C_2H_2$ ,  $H_2O$

Spite: HI,  $H_2^+$ ,  $H^-$ ,  $H_2^-$ , He,  $He^-$ , CI, MgI, AlI, SiI, H and He Rayleigh scattering, electron scattering.

The continuous absorption coefficient will be given by the sum of all contributions:

$$\begin{aligned} \kappa_c = & [[\kappa(H_{bf}) + \kappa(H_{ff}) + \kappa(H_{bf}^-)] (1 - 10^{-\chi_{\lambda} \theta}) \\ & + \kappa(H_{ff}^-) + \dots](1 - \frac{\Theta(H)}{P_e})^{-1} + \kappa(\text{metals}) + \kappa(He_{ff}^-) + \kappa(e) + \dots \end{aligned}$$

where the factor in parenthesis takes into account the ionization of H.

We further note that blanketing effects caused by a large number of small lines will, on the contrary, only decrease the flux, but does not affect the intensity of lines as does the continuous absorption.

## 2.2 Line absorption coefficient

The line absorption coefficient consists of a sum of the contributions of atomic and molecular lines at each wavelength:

### 2.2.1 Atomic lines

$$l = l_{\text{atomic}} + l_{\text{molecular}}$$

The atomic absorption coefficient is defined by:

$$l_{\text{at}} = \frac{\pi e^2}{mc^2} \lambda_o^2 \alpha \text{gf} P_r(n_H) 10^{-\chi_{\text{ex}} \theta} \frac{H(a, v)}{\sqrt{\pi} \Delta \lambda_D} (1 - e^{-hc/\lambda_o kT})$$

where  $P_r(n_H)$  = level populations,  $\alpha$  = element abundance,  $\text{gf}$  = oscillator strength,  $H(a, v)$  = Hjertings profile and other symbols have their usual meaning.

Atomic line lists are of two kinds: (i) identified lines (Moore et al 1966); (ii) computed lines (Kurucz & Peytremann 1975; Kurucz 1981, 1991 (unpublished)). In both cases,  $\text{gf}$ 's are to be fitted to observed spectra: Sun and Arcturus (a metal-poor K giant). Computed line lists contain millions of lines: these are important for the computation of model atmospheres, but most faint lines can be disregarded in spectrum synthesis calculations: as an example, Gaffney & Lester (1991) made tests on the differences caused by eliminating faint lines. At high resolution, identified lines lists are sufficient, however for giants it is convenient to include FeII lines by Kurucz (1981).

### 2.2.2 Molecular lines

The molecular absorption coefficient is defined by:

$$l_{\text{mol}} = \frac{\pi e^2}{m_e c^2} \lambda_{J'J''}^2 f N''_{\text{nvJ}} \frac{H(a, v)}{\sqrt{\pi} \Delta \lambda_D} (1 - e^{-hc/\lambda_{J'J''} kT})$$

where  $f$  = molecular oscillator strength,  $N''_{\text{nvJ}}$  = population of lower level, other symbols as above.

Molecular line lists are available for the most important molecules contributing with strong bands: CN blue and red,  $\text{C}_2$ , CH, TiO, MgH, CaH, NH etc.

Important laboratory work, in particular, by J.G. Phillips & S.P. Davis are greatly useful. Otherwise, the molecular lines can also be computed: shifts in wavelength are not important in the cases of model atmospheres but they have to be corrected in high resolution studies.

### 3. Model Atmospheres

For F, G, K (M) stars, there were available up to recently, the model atmospheres by Gustafsson et al (1975) and Bell et al. (1976) and those by Kurucz (1979). However Kurucz (1979) had no molecules included, whereas the atomic line lists by Gustafsson et al was not as complete as to reproduce the UV spectrum.

Now both sets of models are far better: (i) Kurucz has included molecules and recomputed a new atomic line list of a few million lines, as described in Kurucz (1992); (ii) Gustafsson and collaborators have included the new Kurucz line list in their calculations. One example of the accuracy of the models is shown for the solar spectrum by Kurucz (1992) and Edvardsson et al (1992).

In both cases, the models are plane-parallel, flux constant, assuming LTE, including convection through the mixing-length approximation.

New models have also improved the accuracy of the calculations by introducing an opacity sampling (OS) instead of the original opacity distribution functions (ODF) - see Plez et al (1992).

### 4. Elemental abundances and isotopic ratios

Element abundances can be derived by using curves of growth, or line profiles. Non-blended atomic lines can be used through simple measurement of their equivalent widths; however blended lines and molecular bands are better studied through spectrum synthesis.

#### 4.1 CNO

In particular, the important C, N, O elements can only be derived by using spectrum synthesis of CNO compounded molecules (except for hot stars where atomic lines are present) for C, and N, whereas O abundance determination in cool stars strongly depend on molecular equilibrium and in particular on CO association.

Spectrum synthesis of NH, CH, C<sub>2</sub>, and CN molecular bands are used to derive C and N abundances. NH is a most useful N abundance indicator, but it is located at  $\lambda$  3360 Å of difficult access for faint stars. CH lines at the G-band can be used to derive C abundances (see e.g. Carbon et al 1987). Barbuy et al (1985) show the G-band for BD-18°5550: this halo

star of metallicity  $[\text{Fe}/\text{H}] = -3.0$ , shows no other C abundance indicator, since other lines are too weak.

$\text{C}_2$  bandheads and in particular  $\text{C}_2(0,1) \lambda 5635$  bandhead is also an useful C abundance indicator; finally CN lines can be used to derive N abundances, once the C abundance is known (e.g. Barbuy et al 1991; Milone et al 1992)

Carbon and nitrogen abundances for a large number of stars in the Galaxy were derived through spectrum synthesis by Laird (1985) and Carbon et al (1987).

Oxygen is the key element in chemical evolution models. It is a bona fine primary element, given that it is only produced by massive stars.

A very limited number of oxygen lines are however available. The  $[\text{OI}]\lambda 6300, 6363 \text{ \AA}$  forbidden lines and the  $\text{OI } \lambda (7771.94, 7774.17, 7775.39), (6156.030, 6156.801, 6158.171), (9260.80, 9262.70, 9266.00)$  permitted triplet lines are present in spectra of G-K(M) stars, whereas only the permitted lines are present in B-A-F stars. An additional complication is the NLTE effects, besides other not yet understood mechanism (Kiselman, 1991) that makes the triplet lines to result in false overabundances. (this problem is under study by D. Kiselman). One example is given in Barbuy & Erdelyi-Mendes (1989) where both lines are computed for the star HD 10700, and a difference  $\Delta[\text{O}/\text{Fe}] = 0.15$  is found. Consequently, we dispose practically uniquely of the forbidden lines. In the cooler stars it is important to take into account the molecular association of oxygen in different molecules.

Some results on the oxygen abundances in the Galaxy and in the Magellanic Clouds are discussed below:

*Oxygen in our Galaxy:* Barbuy & Erdelyi-Mendes (1989), Barbuy (1992) and Spite (1992), show  $[\text{O}/\text{Fe}]$  vs  $[\text{Fe}/\text{H}]$  in our Galaxy. The picture of O enrichment in the Galaxy seemed well understood a few years ago: the time lag between supernovae of type II (SNII) and of type I (SNI) causes the O overabundance in the halo, the bulk of Fe being ejected later by SNI. However now details in chemical evolution models require even more precise observations to define, for example: (i) the separation of thick disk and old disk stars; (ii) the metallicity at which the halo  $[\text{O}/\text{Fe}]$  value starts to drop to disk values; (iii) the absolute value in the halo, which should be determined by the mass cut of most massive supernovae (Nomoto & Tsujimoto 1992)

The oxygen abundance in clusters is more difficult to discuss because there may be internal pollution, since cluster stars show a considerable range of O abundances (e.g. Sneden et al 1991, Kraft et al 1992).

*Oxygen abundances in the Magellanic Clouds:* Data points on oxygen abundances for supergiants obtained by Spite & Spite (1992), Spite et al (1993) and Juettner et al (1992),

together with a prediction derived from S/O and Ar/O abundances in planetary nebulae (Freitas Pacheco et al 1993) show a good agreement. A plot of the variation of  $r$  vs  $\epsilon(\text{O})$ , where  $r$  is defined by  $r = \frac{n_{\text{SNII}}}{n_{\text{SNI}} + n_{\text{SNII}}}$  shows that, whereas in our Galaxy the number of SNII relative to SNI decreased along time, in the LMC it was a constant (Freitas Pacheco & Barbuy, this meeting).

#### 4.2 Isotopic ratios

Fainter isotopic lines are shifted close to the main isotopic line. The isotopic effect in atomic lines is not very pronounced, generally  $\Delta\lambda < 0.05 \text{ \AA}$ . The isotopic effect in molecular lines produces larger wavelength shifts.

Considering a molecule as an harmonic oscillator, where the frequency is given by  $\nu = \frac{1}{2\pi} \sqrt{\frac{k}{\mu}}$ , where  $k$  = force constant and  $\mu$  = reduced mass. Therefore:  $\frac{\nu^i}{\nu} = \sqrt{\frac{\mu}{\mu^i}} = \rho$

The molecular energy term is given by the sum of the electronic  $T_e$ , vibrational  $G(v)$  and rotational  $F(J)$  terms. The isotopic shift in the electronic term is negligible.

The vibrational term is given by:  $G(v) = w_e(v+1/2) - w_{ex}e(v+1/2) + \dots$ , where  $v$  = vibrational quantum number,  $w_e$ ,  $w_{ex}e$ .. = anharmonicity constants. The isotopic constants will be given by:  $w_e^i = \rho w_e$ ;  $w_{ex}e^i = \rho^2 w_{ex}e$ ;  $w_{ey}e^i = \rho^3 w_{ey}e$  and the isotopic shift will be finally given by:

$$\nu_{\text{vibr}} = \nu - \nu_i = (1 - \rho)(w_{ev} - w_{ex}e(1 + \rho)v - w_{ey}e(1 + \rho)v^2 + \dots)$$

and so forth for the rotational shift.

Two examples can illustrate it:  $^{12}\text{C}:^{13}\text{C}$  and  $^{24}\text{Mg}:^{25}\text{Mg}:^{26}\text{Mg}$  ratios. The  $^{13}\text{C}(\alpha,n)^{16}\text{O}$  and  $^{22}\text{Ne}(\alpha,n)^{25}\text{Mg}$  reaction seem to be the main sources of neutron enrichment, which explains the interest in the  $^{12}\text{C}:^{13}\text{C}$  and  $^{24}\text{Mg}:^{25}\text{Mg}:^{26}\text{Mg}$  ratios.

CN lines are generally used to derive the  $^{12}\text{C}:^{13}\text{C}$  ratio, although CO overtone bands at  $2.2 \mu\text{m}$  are another possibility (e.g. Schild et al 1992).  $^{12}\text{CN}$  and  $^{13}\text{CN}$  lines at  $\lambda 8004 \text{ \AA}$ , clearly unblended, are used to derive the  $^{12}\text{C}:^{13}\text{C}$  ratio (e.g. Brown et al 1989; Barbuy et al 1992b).

For magnesium, MgH lines are used: (e.g. Tomkin & Lambert 1976, 1979; Barbuy et al 1987, 1992b; Malaney & Lambert 1989). Fig. 1 shows the MgH lines used.

We point out that, whereas low  $^{25,26}\text{Mg}$  have been found in barium stars by Malaney & Lambert (1989) and Barbuy et al. (1992b), these results were recently confirmed by measurements of the reaction rates of the  $^{22}\text{Ne}(\alpha,n)^{25}\text{Mg}$ , where it was shown that in fact this reaction is less efficient than previously thought (Hammer et al 1992).

Only a few authors have developed work on isotopic ratios, however it may lead to important answers regarding nucleosynthesis.

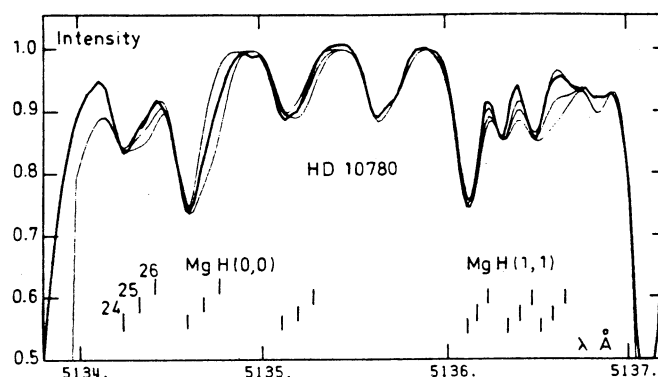


Fig. 1 - <sup>24,25,26</sup>MgH lines used to derive Mg isotopic ratios (cf. Barbuy et al 1987)

## 5. T Tauri stars and Li-rich giants

A low veiling spectrum can be de veiled by correcting the lines relative to a normal K dwarf, and a detailed analysis can be carried out as for a normal K dwarf. Fig. 2 illustrates a de-veiling procedure.

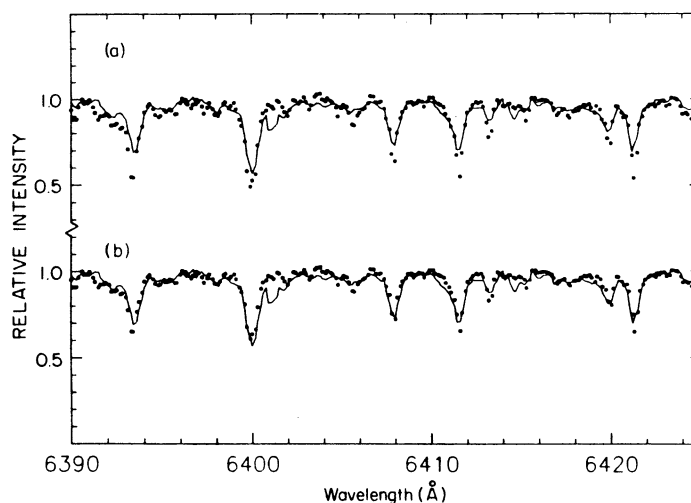
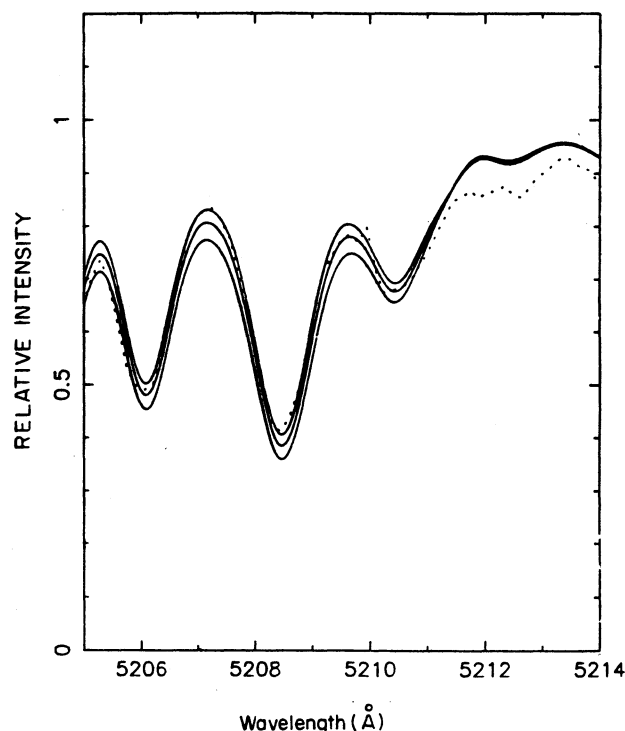


Fig. 2 - De-veiling: (a) T Tauri star Sz98 plotted over an Hyades K7 dwarf; (b) Hyades star where a 0.3 de-veiling is applied compared to the original spectrum. Symbols: open dots: Hyades, solid lines: Sz98 (from Batalha et al 1992)

Synthetic spectra of molecular bands such as MgH, CN and in particular CaH can be applied in order to check the temperature and gravity used. Fig. 3 shows the MgH line computed for different values of the gravity.



**Fig. 3 - MgH(0,0) bandhead at  $\lambda 521.1$  nm for the T Tauri star Sz06 computed with  $\log g = 3.7, 3.9, 4.1$ , Symbols: dotted line: observed spectrum, solid lines: synthetic spectra (from Batalha et al 1992)**

## **6. A grid of synthetic spectra for the derivation of stellar parameters in F,G,K stars**

The study of stellar populations in a given direction in the Galaxy, requires the study of stars at large distances where high resolution spectroscopy is not possible. Besides, due to the large number of stars studied it is necessary to rely on some method to determine stellar properties. Generally photometry has been used. We have started a program to study stellar populations using low resolution spectra. For deriving the stellar parameters, a grid of 700 synthetic spectra was generated in the wavelength region  $\lambda\lambda$  4780-5300 Å, and a code for identifying stellar parameters was written.

The method to derive stellar parameters can be summarized as follows: The observed spectrum is divided by the spectrum of a reference star. The resulting signal  $\delta f(\lambda) = \log F_*/F_{ref}$  is then used, in conjunction with the grid of synthetic spectra, to derive the final parameters, through a perturbation method. In order to identify the signature of a temper



ature difference, two synthetic spectra are used, one close to the standard star, and another of temperature different by  $\delta T_{eff}$ , the gravity and metallicity remaining the same. The logarithm of the ratio of fluxes between these synthetic spectra gives a signal corresponding to a perturbation in temperature ( $\delta f_{T_{eff}}(\lambda)$ ). The same is done for the gravity and for the metallicity, where perturbations  $\delta f_{logg}(\lambda)$  and  $\delta f_{[M/H]}(\lambda)$  are found.

The signal error  $\delta f(\lambda)$  is expressed as a linear combination of  $\delta f_{T_{eff}}(\lambda)$ ,  $\delta f_{logg}(\lambda)$  and  $\delta f_{[M/H]}(\lambda)$ , with a constant and a linear function of  $\lambda$ , with a constant and a linear function of  $\lambda$  added, to account for scale factors and possible interstellar reddening:

$$\delta f(\lambda) = a\delta f_{T_{eff}}(\lambda) + b\delta f_{logg}(\lambda) + c\delta f_{[M/H]}(\lambda) + d(\lambda - \lambda_o) + e$$

The method is such that, through the use of the grid, the coefficients of the linear combination which give a minimum error are found by the least squares fit.

Finally, differences in temperature  $\Delta T_{eff} = a\delta T_{eff}$ , gravity  $\Delta \log g = b\delta \log g$ , and metallicity  $\Delta [M/H] = c\delta [M/H]$  between the program star and the reference star are established. Figs. 3 in Cayrel et al (1991b) illustrate the method: in the upper panel is the best-fitting synthetic spectrum to an observed star, and in the bottom panel is plotted the result of dividing the observed program star by the respective best-fitting synthetic ones.

Up to now, our conclusion is that extremely metal-poor giants are less numerous than predicted by the standard Bahcall-Soneira (1985) Galaxy model (Cayrel et al 1991a,b).

## 7. Strong features in composite spectra

In the integrated spectra of normal galaxies only a few strong features are seen. This is mainly due to the internal velocity dispersions (of the order of  $\sim 200 \text{ km s}^{-1}$ ) which broaden the lines, so that even if we could observe galaxies at high resolution, no individual spectral lines would be seen. The main features detected are: Hydrogen lines; 'Fe'5270, 'Fe'5335 among other 'metallic' blends; CaII H,K lines ( $\lambda 3968.49$ ,  $\lambda 3933.68 \text{ \AA}$ ); G-band (CH bandhead at  $\lambda 4314 \text{ \AA}$ ); MgI triplet lines ( $\lambda 5167.33$ ,  $\lambda 5172.7$ ,  $\lambda 5183.62 \text{ \AA}$ ); NaD doublet ( $\lambda 5885.94$ ,  $\lambda 5889.97 \text{ \AA}$ ); TiO bands at  $\lambda 6200$ ,  $\lambda 7300 \text{ \AA}$ ; NaI doublet ( $\lambda 8183.25$ ,  $\lambda 8194.84 \text{ \AA}$ ); CaII triplet ( $\lambda 8498.06$ ,  $\lambda 8542.14$ ,  $\lambda 8662.17 \text{ \AA}$ ).

In order to compute these features, large spectral regions have to be synthesized ( $> 400 \text{ \AA}$ ). Our efforts in the last years have been concentrated in reproducing these main features, in particular the MgI triplet, the CaII triplet and the TiO bands.

### 7.1 Integrated spectra of composite systems

Assuming that the bulge of elliptical and lenticular galaxies are similar, in terms of stellar populations, to our Galactic bulge, we use as a key reference the bulge globular clusters. In

order to build composite spectra of metal-rich populations, we have used the information contained in the BVRI colour-magnitude diagrams (CMDs) of the galactic bulge globular clusters NGC 6553 (Ortolani, Barbuy & Bica 1990), NGC 6528 (Ortolani, Bica & Barbuy 1992), Terzan 1 (Ortolani, Bica & Barbuy 1993), combined with the spectroscopic abundance determination of the stellar parameters for NGC 6553 (Barbuy et al 1992a), and the relative positions of CMDs of metal-rich clusters by Bica, Barbuy & Ortolani (1991). We adopted for our basic derivations the globular cluster NGC 6553, which shows nearly solar metallicity:  $[M/H] \approx -0.2$ . The CMDs of NGC 6553, NGC 6528 and Terzan 1 present the following main peculiarities: (a) the red giant branch (RGB) turns over, in such a way that the RGB tip has a luminosity as low as that of the horizontal branch (HB); (b) a colour shift occurs as a function of increasing metallicity; (c) the magnitude of brighter giants is lower than those of metal-poor clusters by  $\Delta V > 1$  mag. Further information used from CMDs is: (i) the relative number of stars in each evolutionary stage was directly counted on the CMDs; (ii) the temperatures were derived as described in Barbuy et al (1992a).

The composite spectra were built by adding up the synthetic spectra of the different evolutionary stages, weighted by their relative numbers and relative fluxes.

A major effort has been applied up to now in reproducing integrated spectra of lenticular and elliptical galaxies in the MgI triplet region: we have built libraries of synthetic spectra for  $[M/H] = -1.0, -0.5$  and  $0.0$ , each one containing 10 evolutionary stages.

The comparison of the composite spectra to observed spectra is shown in Fig. 4.

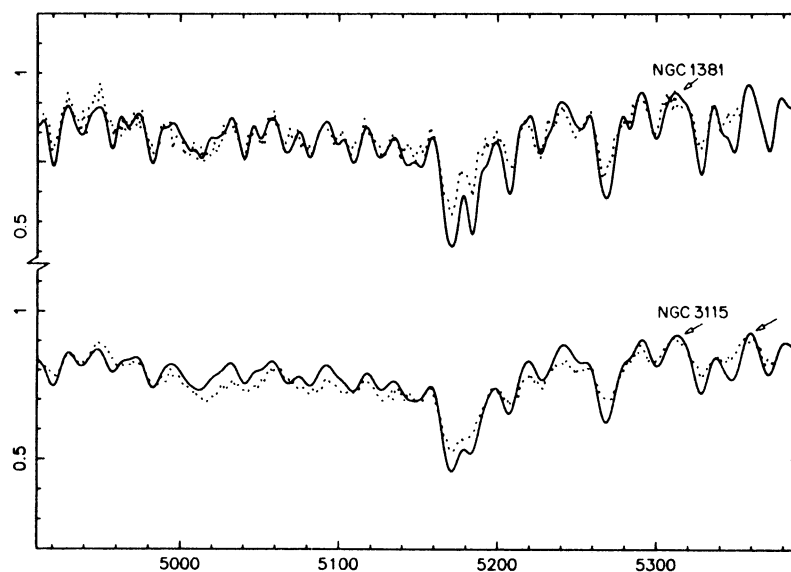


Fig. 4 - Fit of composite synthetic spectra (solid lines) to observed spectra (dotted lines) for NGC 1381, NGC 3115 (cf de Souza et al 1992)

## References

- Bahcall, J.N., Ratnatunga, K.U., Buser, R., Fenkart, R.P., Spaenhauer, A.: 1985, ApJ 299, 616
- Barbuy, B.: 1982, PhD thesis, Université de Paris VII
- Barbuy, B.: 1992, in *The Stellar Populations of Galaxies*, IAU Symp 149, eds. B. Barbuy, A. Renzini, Kluwer Acad. Pub. (Dordrecht: Holland), 143
- Barbuy, B., Spite, F., Spite, M.: 1985, A&A 144, 343
- Barbuy, B., Spite, F., Spite, M.: 1987, A&A 178, 199
- Barbuy, B., Erdelyi-Mendes, B.: 1989, A&A 214, 239
- Barbuy, B., Spite, M., Spite, F., Milone, A.: 1991, A&A 247, 15
- Barbuy, B., Castro, S., Ortolani, S., Bica, E.: 1992a, A&A 259, 607
- Barbuy, B., Jorissen, A., Rossi, S., Arnould, M.: 1992b, A&A 262, 216
- Batalha, C., Gregorio-Hetem, J., Barbuy, B.: 1992, in preparation
- Bell, R.A., Eriksson, K., Gustafsson, B., Nordlund, A.: 1976, A&AS 23, 37
- Bica, E., Barbuy, B., Ortolani, S.: 1991, ApJ 382, L15
- Brown, J.A., Wallerstein, G.: 1989, AJ 98, 1643
- Brown, J.A., Sneden, C., Lambert, D.L., Dutchover, E.: 1989, ApJS 71, 293
- Carbon, D., Barbuy, B., Kraft, R., Friel, E., Suntzeff, N.: 1987, PASP 99, 335
- Cayrel, R., Perrin, M.-N., Barbuy, B., Buser, R.: 1991, A&A 247, 108
- Cayrel, R., Perrin, M.-N., Buser, R., Barbuy, B., Coupry, M.-F.: 1991, A&A 247, 122
- Cayrel, R., Perrin, M.-N., Boulon, J., Barbuy, B., Bienaymé, O., Friel, E.: 1993, in preparation
- Edvardsson, B., Andersen, J., Gustafsson, B., Lambert, D.L., Nissen, P., Tomkin, J.: 1992, in preparation
- Freitas Pacheco, J.A.: 1993, ApJ, in press
- Freitas Pacheco, J.A., Barbuy, B., Costa, R.D.D., Idiart, T.: 1993, A&A, in press
- Gaffney, N.I., Lester, D.F.: 1992, ApJ 394, 139
- Gustafsson, B., Bell, R.A., Eriksson, K., Nordlund, A.: 1975, A&A 42, 407
- Hammer, J.W., Drotleff, H.W., Denker, A., Knee, H., Soiné, M., Wolf, G., Greife, U., Rolfs, C., Trautvetter, H.-P.: 1992, in *Nuclei in the Cosmos II*, ed. F. Käppeler, to appear
- Juettner, A., Stahl, O., Wolf, B., Baschek, B.: 1992, in "New Aspects of Magellanic Clouds Research", ed. G. Klare, Springer, in press

- Kraft, R., Sneden, C., Langer, G.E., Prosser, C.: 1992, AJ 104, 645
- Kiselman, D.: 1991, A&A 245, L9
- Kurucz, R., Peytremann, E.: 1975, SAO Report n° 362
- Kurucz, R.: 1979, ApJ 40, 1
- Kurucz, R.: 1981, SAO Report n° 390
- Kurucz, R.: 1992, in *The Stellar Populations of Galaxies*, IAU Symp 149, eds. B. Barbuy, A. Renzini, Kluwer Acad. Pub. (Dordrecht: Holland), 225
- Laird, J.: 1985, ApJ 289, 556
- Malaney, R., Lambert, D.L.: 1989, MNRAS 235, 695
- Milone, A., Barbuy, B., Spite, M., Spite, F.: 1992, A&A 261, 551
- Moore, C.E., Minnaert, M.G., Houtgast, J.: 1966, NBS Monograph n° 61
- Nomoto, K., Tsujimoto, T.: 1992, in *Nuclei in the Cosmos.II*, ed. F. Käppeler, to appear
- Ortolani, S., Barbuy, B., Bica, E.: 1990, A&A 236, 362
- Ortolani, S., Bica, E., Barbuy, B.: 1992, A&AS 92, 441
- Ortolani, S., Bica, E., Barbuy, B.: 1993, A&A, in press
- Plez, B., Brett, J.M., Nordlund, A.: 1992, A&A 256, 551
- Schild, H., Boyle, S.J., Schmid, H.M.: 1992, MNRAS 258, 95
- Sneden, C., Kraft, R., Prosser, C., Langer, G.: 1991, AJ 102, 2001
- de Souza, R., Barbuy, B., dos Anjos, S.: 1992, AJ, submitted
- Spite, M.: 1967, Ann. Astrophys. 30, 211
- Spite, M.: 1992, in *The Stellar Populations of Galaxies*, IAU Symp. 149, eds. B. Barbuy & A. Renzini, Kluwer Acad. Publ. (Dordrecht: Holland), 123
- Spite, M., Spite, F.: 1992, in "New Aspects of Magellanic Clouds Research", ed. G. Klare, Springer, in press
- Spite, F., Spite, M., Barbuy, B.: 1992, A&A, submitted
- Tomkin, J., Lambert, D.L.: 1976, ApJ 208, 436
- Tomkin, J., Lambert, D.L.: 1979, ApJ 227, 209

Beatriz Barbuy, IAG-USP, Depto de Astronomia, CP 9638, São Paulo 01065-970, Brazil.